PERGAMON

Vision Research 41 (2001) 1023–1037

Vision Research

www.elsevier.com/locate/visres

Dynamics of contour integration☆

Robert F. Hess *, William H.A. Beaudot, Kathy T. Mullen

Department of Ophthalmology, McGill Vision Research, McGill University, 687 Pine Avenue West (H4-14), Montréal, Québec, Canada H3A 1A1

Received 3 May 2000; received in revised form 6 October 2000

Abstract

To determine the dynamics of contour integration the temporal properties of the individual contour elements were varied as well as those of the contour they form. A temporal version of a contour integration paradigm (Field, D. J., Hayes, A., & Hess, R. F. (1993) *Vision Research*, 33, 173–193) was used to assess these two temporal dynamics as a function of the contrast of individual elements and the curvature of the contour. The results show that the dynamics of contour integration are good when the contrast of the individual elements is modulated in time (10–30 Hz), but are poor when contour linking per se is temporally modulated (1–12 Hz). The dynamics of contour linking is not dependent on the absolute contrast of the linking elements, so long as they are visible, but does vary with the curvature of the contour. For straight contours, temporal resolution is around 6–12 Hz but falls to around 1–2 Hz for curved contours.

Keywords: Contour integration; Temporal sensitivity; Dynamics; Curvature; Contrast

1. Introduction

There is a growing awareness of the importance of network interactions within the visual cortex as opposed to the purely local properties of the classical receptive field. This is especially true for the integration of visual contours for which the concept of an 'association field' has been developed in an attempt to define the functional nature of the underlying lateral interactions (Field, Hayes, & Hess, 1993). According to this psychophysical approach, extended contours composed of elements that are co-oriented and co-aligned are most detectable, following the Gestalt rule of good continuation (for review see Kovacs, 1996; Hess & Field, 1999). Anatomical and physiological support for the psychophysically defined association field comes from a number of studies (e.g. Rockland & Lund, 1982; Gilbert & Wiesel, 1983; Malach, Amir, Harel, & Grinvald, 1993; Bosking, Zhang, Schofield, & Fitzpatrick, 1997) that delineate how cells within ocular dominance columns are interconnected across disparate regions of cortex through long-range connections. There is now neurophysiological evidence that these network interactions are context-dependent (e.g. Lamme, Super, & Spekreijse, 1998), which in turn suggests that the saliency of a stimulus can be modulated according to its global properties (Fregnac, Bringuier, Chavane, Glaeser, & Lorenceau, 1996; Gilbert, Das, Ito, Kapadia, & Westheimer, 1996; Toth, Rao, Kim, Somers, & Sur, 1996; Gilbert, 1997; Kapadia, Westheimer, & Gilbert, 1999; Lorenceau & Zago, 1999; Pettet, 1999; Polat, 1999). Recent experiments on figure-ground segregation, an area closely related to contour integration, suggest that intra- as well as extra-cortical feedback circuits are involved in these network interactions (Burkhalter, 1993; Gilbert, 1996, 1998; Hupé, James, Payne, Lomber, Girard, & Bullier, 1998; Lamme et al., 1998).

A great deal is known about the spatial properties of this network interaction from psychophysical studies (for review see: Kovacs, 1996; Hess & Field, 1999), however, very little is known about the temporal properties or dynamics involved in the orientation linking of extended contours. The little we know relates to the importance of temporal synchrony between path and background elements (Usher & Donnelly, 1998; Beau-

☆ This work was initially reported to the 2000 Meeting of the Association for Research in Vision and Ophthalmology, Fort Lauderdale, FL, USA (IOVS 41/4, S441).

* Corresponding author. Tel.: +1-514-8421231, ext. 4815; fax: +1-514-8431691.

E-mail address: rhess@bradman.vision.mcgill.ca (R.F. Hess).

0042-6989/01/$ - see front matter
PII: S0042-6989(01)00020-7

dot, forthcoming), the effect of the relative separation of path and background elements on processing time (Braun, 1999) and how reaction times depend on contour contrast, curvature and chromaticity (Beaudot & Mullen, forthcoming). Though these are important issues we still do not know for example whether the association field is dynamic or fixed or whether its dynamics depends on the curvature, luminance contrast or contrast polarity of the contour.

Furthermore, a knowledge of the dynamics of contour integration may bear upon whether a temporal code is used to link the outputs of the neurons at early stages of cortical processing. Consider two extreme examples of a temporal code for contour linking: temporal synchronization and temporal sequencing. According to the first hypothesis, for which there is evidence both for (Fahle, 1993; Blake & Yang, 1997; Alais, Blake, & Lee, 1998; Usher & Donnelly, 1998; Lee & Blake, 1999) and against (Golledge, Hilgetag, & Tovee, 1996; Kiper, Gegenfurtner, & Movshon, 1996; Hardcastle, 1997; Lamme & Spekreijse, 1998; Ziebell & Nothdurft, 1999), temporal oscillatory synchronization in the firing pattern of individual cortical cells could be the substrate for perceptual binding (e.g. Singer & Gray, 1995), and consequently for contour integration (Roelfsema & Singer, 1998; Yen & Finkel, 1998). Since the temporal resolution of this synchronization is high, in the Gamma band (i.e. around 40 Hz), if only a few cycles are needed for this posited linking code, one would expect that the temporal resolution of contour integration as a whole to be high.

According to the temporal sequencing hypothesis, figure-ground discrimination requires feedback from higher visual areas (Burkhalter, 1993; Zipser, Lamme, & Schiller, 1996; Hupé et al., 1998; Lamme et al., 1998) as well as long-range lateral connections within the one cortical region (Gilbert & Wiesel, 1989; Atkinson & Braddick, 1992; Burkhalter, 1993; Gilbert et al., 1996; Lamme et al., 1998). As a possible consequence, different parts of the cellular spike train may reflect different aspects of visual processing, with the early part of the spike-train carrying the code for contrast and the latter part, the code for contour/figure-ground (Lamme, 1995; Zipser et al., 1996). Such a mechanism would predict that the detection of a contour per se, and more generally a 'context-defined feature', would have slower dynamics compared with the mainly feedforward effects, for example, in the signaling of contrast (Richmond, Gawne, & Jin, 1997; Hess, Dakin, & Field, 1998; Lamme et al., 1998).

These issues point to the potential importance of the dynamics of contour integration about which we know so little. To redress this, we have assessed the dynamics of contour integration by not only temporally varying the contrast of the elements constituting the contour as in previous, related, texture-segregation studies, but also by temporally varying the linking itself. The results show that the linking process is slow compared with the temporal properties for the detection of the constituent elements, and that the dynamics of linking varies with contour curvature but not with the contour contrast.

2. Methods

2.1. Stimuli

The stimuli were square patches ($14 \times 14°$) of pseudo-randomly distributed Gabor elements (Fig. 1A, left panel). The subject's task was to detect a 'path' which consisted of a set of ten oriented Gabor elements aligned along a common contour, embedded in the background of similar but randomly oriented Gabor elements. Inspection of Fig. 1A reveals that the path in the example winds horizontally across the figure. Gabor elements were used to limit the spatial bandwidth of the stimuli (Field et al., 1993; McIlhagga & Mullen, 1996). The elements were odd symmetric and defined by the equation:

$$g(x, y, \theta) = c \sin(2\pi f(x \sin\theta + y \cos\theta)) \exp -\left(\frac{x^2 + y^2}{2\sigma^2}\right) \quad (1)$$

where θ is the element orientation in degrees, (x, y) is the distance in degrees from the element center, and c is the contrast. The sinusoidal frequency (f) is 1.5 cpd, and the space constant (σ) is 0.17°.

A temporal 2AFC task was used to measure the subject's ability to detect the path, in which the choice was between the path stimulus and a no-path stimulus consisting only of randomly placed Gabor elements. The no-path stimulus was constructed with the following algorithm; the stimulus area was divided into a 14×14 grid of equally sized cells (each 1° square) and a Gabor element of random orientation was placed in each cell with the restriction that each cell contained the center of only one Gabor element. This pseudo-random placement prevents clumping of the elements. Overlap of the elements was also prevented by restricting the placement of their centers within the cell. It was sometimes impossible to place a Gabor element in its cell because it would be too close to elements previously placed. This produced an empty cell, and no more than eight empty cells were permitted in a display and the average number was 4. The average distance between neighboring Gabor elements was 1.3°.

The path stimulus can be considered as two parts, the ten path elements themselves and the background

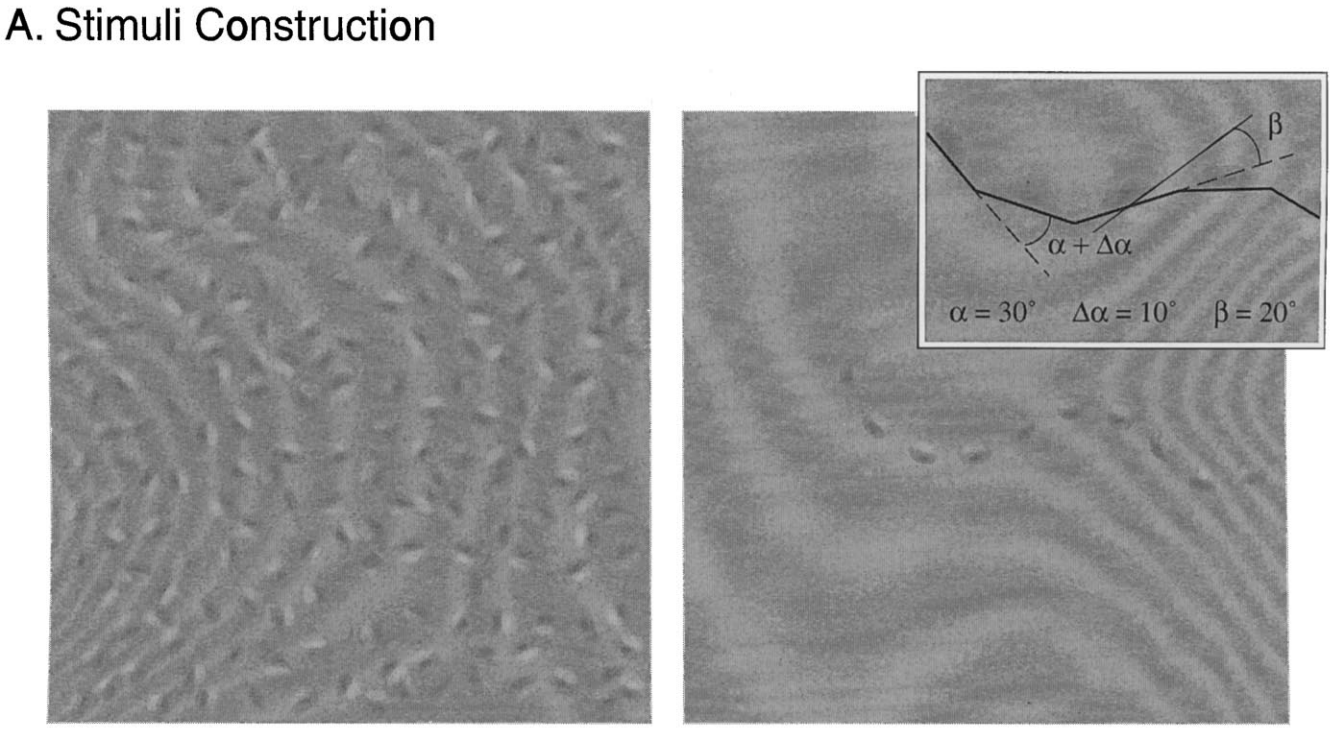
A. Stimuli Construction
β
α + Δα
α = 30° Δα = 10° β = 20°
B. Orientation Masking
Forward Mask
(500 ms)
Test
(variable duration)
Backward Mask
(500 ms)

Fig. 1.

C. Stimuli sequence in the oriention modulation experiment

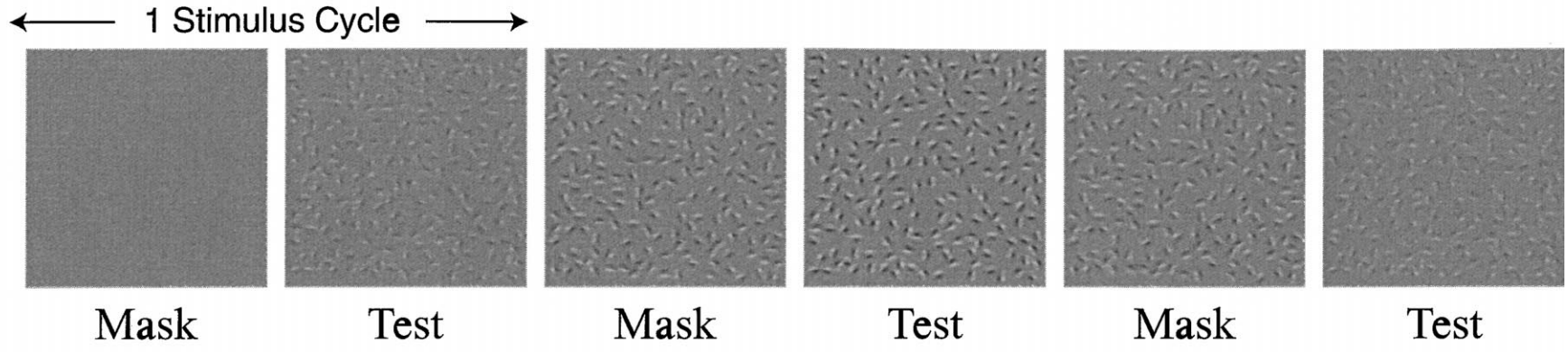

D. Basic stimuli used in the contrast modulation experiment

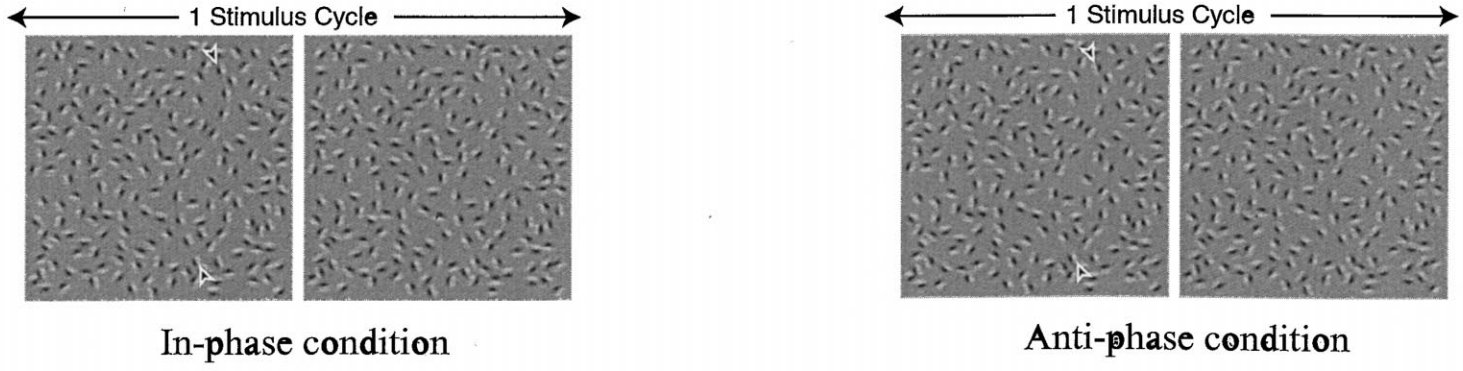

Fig. 1. (*Continued*)

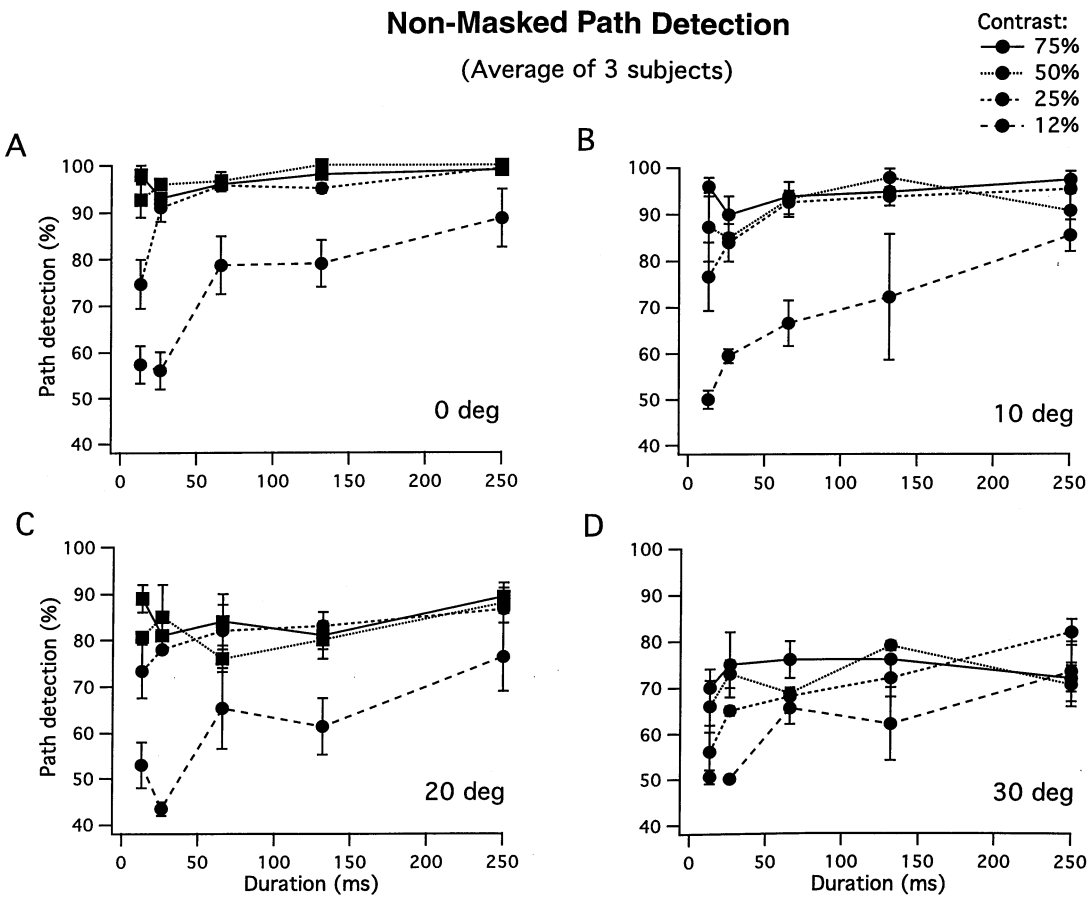

Fig. 2. Effect of contrast and curvature on path detection as a function of stimulus duration in the non-masked condition. Each data point represents performance averaged across the three subjects. Each subject performs one or two sessions of 50 trials per data point. Error bars denote S.D.

elements. A subset of path elements is shown in Fig. 1A, right panel, and its construction is illustrated in the inset. The path has a 'backbone' of ten invisible line segments, and each line segment is randomly selected to be between 1.2 and 1.4° long. The shape of the backbone is controlled by the parameter α (termed path curvature) which determines the angle difference between adjacent backbone elements. Higher values of α produce more curvature in the path, and lower values produce straighter paths. Primarily to avoid the occurrence of straight paths when α is 0°, an orientation jitter ($\Delta\alpha$) uniformly distributed between $\pm 10°$ was added to the path curvature. Gabor elements were placed in the middle of each backbone segment with the same orientation. β gives the orientation of the Gabor element with respect to the backbone element. β is zero in experiments presented in this paper. Finally, to avoid

Fig. 1. (A) *Left panel*: An example of the stimulus. The 'path' is difficult to detect when embedded in a background of similar but randomly oriented elements. Experienced subjects perform at around 65–75% correct under a steady presentation of 500 ms. *Right panel*. The path is shown separated from the background elements. It is a chain of ten Gabor elements which vary systematically in their orientation, as described in the inset. *Inset:* The path is made up of ten backbone line segments. The orientation difference between each successive line segment is given by the angle α which in this case is $\pm 30°$. α determines the path curvature. $\Delta\alpha$ is a small orientation jitter added to α and is uniformly distributed between $\pm 10°$. β gives the orientation of the Gabor element with respect to the backbone element. β is zero in experiments presented in this paper. (B) Sequence of stimuli presented in a trial of the masked condition in the first group of experiments, and repeated cyclically in the second group of experiments. Forward mask and backward mask are identical, and built from the orientation randomization of each Gabor element composing the test stimulus. Extremities of the 20° path are denoted by white arrows in the test stimulus. (C) Example of stimuli sequence presented in a path interval of the orientation modulation experiment. A stimulus cycle is composed of a test stimulus and its associated orientation mask presented for the same duration (in this particular example we used the stimuli shown in B). This stimulus cycle is repeated over one second, and the contrast of the whole stimulus is modulated by a centred Gaussian window. (D) Examples of stimuli presented in a path interval of the contrast modulation experiment. In both in-phase and anti-phase conditions, a stimulus cycle is composed of a test stimulus and its contrast-reversed counterpart. The whole stimulus is built identically to the one of the orientation modulation experiment: cyclic presentation over 1 sec with a Gaussian contrast modulation. Arrows indicate extremities of the 20° paths.

random closure of the paths with a high curvature, which can affect detection (Elder & Zucker, 1993; Kovacs & Julesz, 1993), paths which looped back on themselves were discarded and new ones generated. The entire path was pasted into the display at a random location, making sure that the centers of the Gabor elements occupied different cells, and that at least one path element passed through the central region of the stimulus (defined as a circular region 3° in diameter). The remaining empty cells were filled with randomly oriented Gabor elements, as in the no-path stimulus.

Various control measurements ensured that no spurious cues could be used for path detection. In particular it was ascertained that the presence of the path does not affect the local densities of the elements since the averaged distance between path elements and between background elements is the same and the number of empty neighboring cells are the same for both path and background elements. Furthermore, the number of empty cells is the same for both path and no-path stimuli indicating no global density changes. If neither density nor proximity are cues, path visibility should be due only to the alignment of the elements of the path since nothing else distinguishes path element from background element. This was confirmed in a control experiment in which the orientation of the path elements was randomized. The path could not be detected under extended viewing regardless of the curvature. The continuity in the local orientation across space is then a crucial feature for path detection.

2.2. Apparatus and calibrations

Stimuli were displayed on a Sony Trinitron monitor driven by a VSG 2/4 graphics board (Cambridge Research Systems) with 15 bits contrast resolution, housed in a Pentium PC computer. The frame rate of the display was 76 Hz. The monitor was gamma corrected in software with lookup tables using luminance measurements obtained from a United Detector Technology Optometer (UDT S370) fitted with a 265 photometric sensor. The monitor was viewed in a dimly lit room. The mean luminance of the display was 14.2 cd/m^2. The stimuli were viewed at 60cm, and subtended a constant area of $14 \times 14°$.

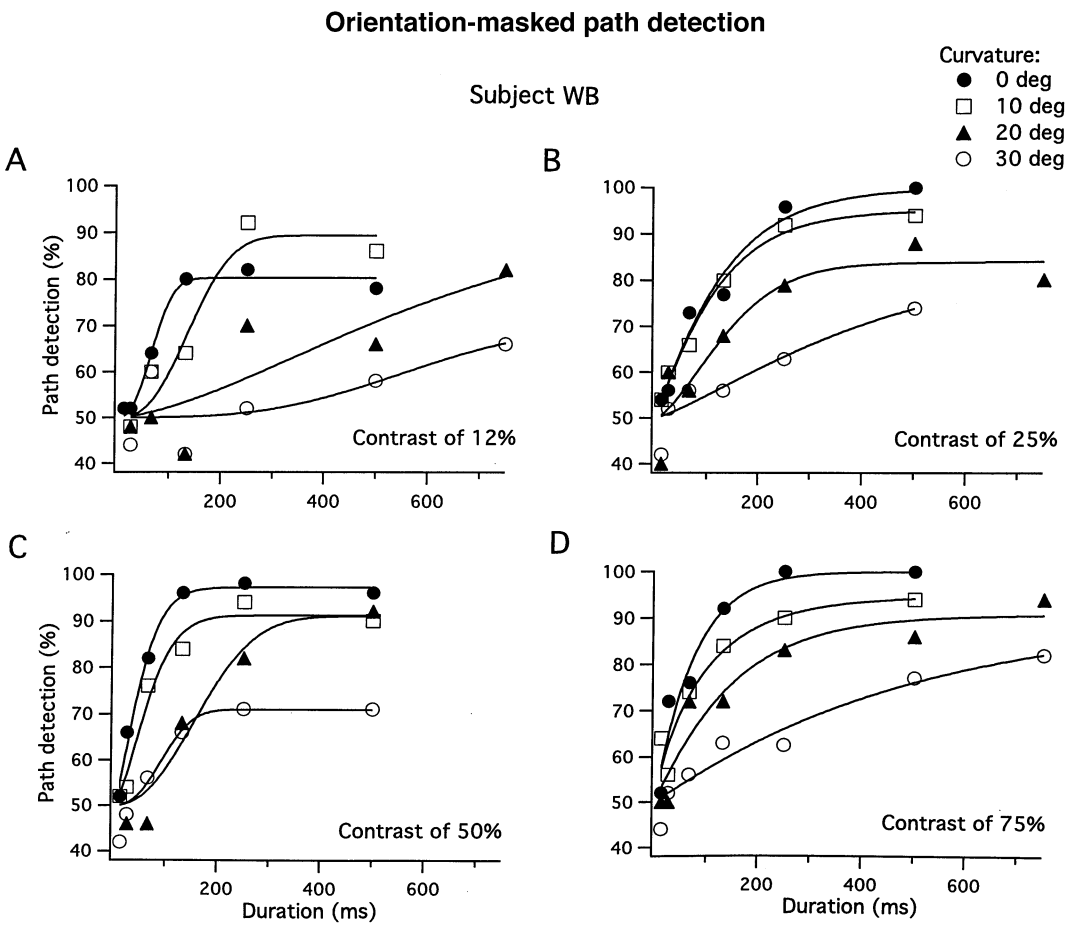

Fig. 3. Effect of curvature and contrast on path detection as a function of stimulus duration in the orientation-masked condition. Data shown for one subject (WB), the other two subjects show similar results. Each subject performs one or two sessions of 50 trials per data point. Filled and open symbols represent performance measurement (% correct). Solid lines denote fits to Eq. (2) to each data set.

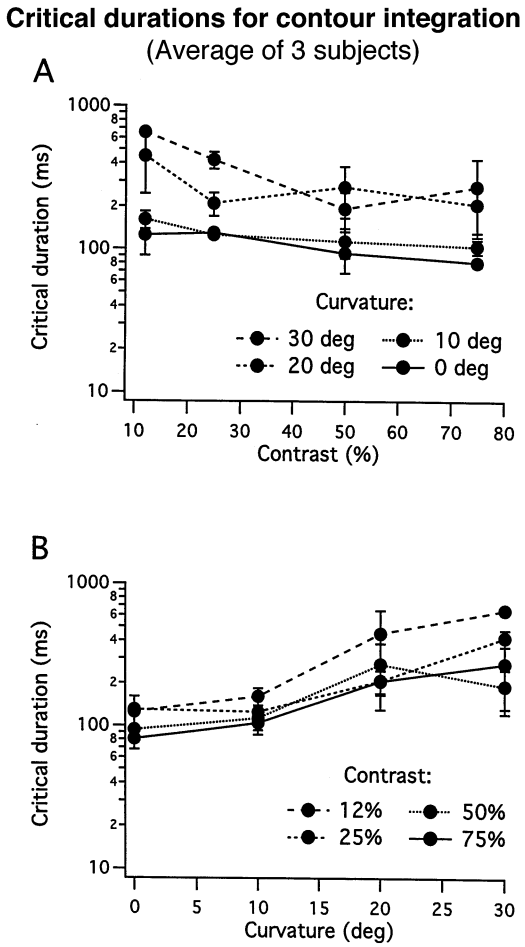

Fig. 4. Critical durations derived from the fits shown in Fig. 3. Time constants: (A) as a function of contrast for each curvature; (B) as a function of curvature for each contrast. Each data point represents the mean of the fits for the three subjects. Error bars denote S.D.

2.3. Protocol

A temporal 2AFC paradigm was used in all experiments to measure the subject's ability to detect the path, in which the choice was between a contour path stimulus and a no-path stimulus. Each trial consisted of this pair of stimuli presented sequentially for the same duration. Presentations were abrupt with a 0.5 s inter-stimulus interval. The inter-stimulus interval was spatially homogeneous with the same mean luminance than stimuli presented during test intervals. After each trial the subject indicated the interval perceived as containing a path by pressing the appropriate mouse button. The number of trials per session for each experiment was 50 for each subject, and 1–3 sessions were performed for each condition. Feedback was given. A small fixation mark appeared in the centre of the display during the whole session. Stimuli were generated on-line, and a new stimulus was generated for each presentation.

In separate experiments, the duration of stimulus presentation, temporal frequency of contrast modulation, and temporal frequency of element orientation modulation were varied, and within each experiment, the effects of curvature and contrast were measured. The first group of experiments investigated the effects of stimulus duration, and two conditions were used. In the first, the test stimulus was presented for a variable duration, preceded and followed by a blank field of the same mean luminance. The second condition was a masked condition designed to prevent path integration continuing beyond the interval containing the test stimulus. In this condition, the test stimulus in each trial was masked with stimuli presented both before and after it for the same duration (sandwich masking). The masks consisted of arrays of Gabor elements placed identically to those of the test stimulus with a random change in their orientations in the range $\pm[45-135]°$ (Fig. 1B). Duration was varied between 13 and 750 ms.

In the second group of experiments, one looked at the effect on path detection of temporally modulating the orientation of individual Gabor elements. The orientation of all elements in the array was changed in successive presentations over a duration of 1 s. The stimuli were derived from the masked condition of the first group of experiments: the orientation modulation was constructed from the temporal succession of the test path stimulus and the masking no-path stimulus for a duration of 1 s at a given rate. The effect of this procedure is to modulate the path elements in and out of alignment without altering either their location or relative contrast. Modulation rate was varied from 0.5 to 19 Hz. The overall contrast of each presentation of these orientation- altered stimuli was Gaussian enveloped with a sigma of 500 ms centred on the temporal window (1 s).

In the third group of experiments, one looked at the effect of temporal contrast modulation on detection of paths composed of in-phase and anti-phase Gabor patches, respectively. Protocol and stimulus properties were identical to those in the second group of experiments, except that the orientation mask was replaced by a stimulus identical to the test stimulus with opposite contrast polarity. This makes all Gabor patches of the stimuli alternate in their contrast polarity each stimulus frame. In the in-phase condition, each frame composing the flickering path stimuli sequence contains a path made of Gabor patches with the same contrast polarity across space. In the anti-phase condition, each frame composing the flickering path stimuli sequence contains a path made of Gabor patches with alternating contrast polarity across space.

The subjects repeated experiment 2 with smooth (30° curvature) and closed contours (smooth curvature of 36° for ten elements) composed of Gabor elements with 50% contrast. A smooth contour differs from a jagged

one in that the angle between individual elements along the contour is of the same sign.

2.4. Observers

The observers were the three authors (WB, RFH & KTM). All have normal, or refracted to normal vision. All experiments were done under binocular conditions.

3. Results

3.1. The roles of contrast and curvature on critical duration

In the first experiment the dynamics of contour integration were investigated by varying the time the stimulus was presented. This was done with and without a post stimulus mask to ensure that visual processing was limited to the interval during which the stimulus was presented. Thus the combined effects of the duration of stimulus presentation, contrast, and path curvature in limiting contour integration in the masked and unmasked conditions were measured. Path detection was measured over a range of durations (13–250 ms without mask, 13–750 ms with mask), contrasts (suprathreshold range, 12–75%), and path curvatures (0–30°). Results are shown in Figs. 2 and 3 by data points, solid curves in Fig. 3 denote fits as described below. Each curve represents performance on path detection as a function of duration for different contrasts and curvatures.

Data for the non-masked condition (Fig. 2) is averaged across the three subjects. It shows that, apart from an initial steep rise at the shortest duration (13 ms), performance is almost constant with duration (except for the lowest contrast 12% which is more dependent on duration). However the overall level of this asymptotic performance decreases progressively with the curvature of the contour. Friedman's two-way ANOVAs of asymptotic performance levels (data accumulated across duration because duration has no influence on performance, except for the lowest contrast) for both contrast and curvature conditions confirm that there is no significant difference in performance between the three suprathreshold contrast conditions (25, 50 &75%), and that the loss of asymptotic performance with curvature is significant ($X^2_F = 82.456$, $df = 3$, $P < 0.0001$, $N = 45$), following previous studies (Field et al., 1993; Mullen, Beaudot, & McIlhagga, 2000). This first experiment demonstrates that contour integration can be effectively performed even for the shortest duration (13 ms) and that these fast *dynamics* do not appear to depend on the curvature of the contour.

Results for the masked condition are shown in Fig. 3; representative data for only one of the three subjects tested is shown. There is a shallower initial dependence on stimulus duration than in the unmasked condition. These curves also show that the asymptotic level and the steepness of the initial dependence on duration decrease with curvature. To derive a critical duration (i.e. a time constant), we fitted the data of Fig. 3 (performance as a function of duration at each path curvature and each contrast) with Weibull functions corrected to take the differing asymptotic performance levels into account:

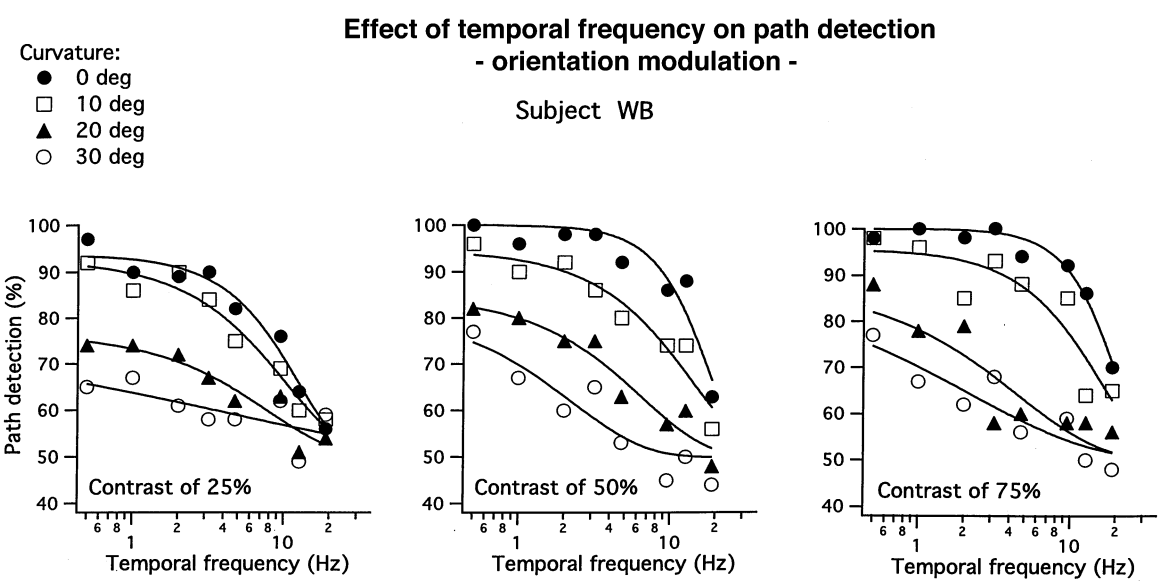

Fig. 5. Effect of curvature and contrast on path detection as a function of stimulus temporal frequency in the temporal orientation modulation experiment. Data shown for one subject (WB), other subjects show similar results. Each subject performs one to three sessions of 50 trials per data point. Filled and open symbols represent performance measurement (% correct). Solid lines denote fits to Eq. (3) for each data set.

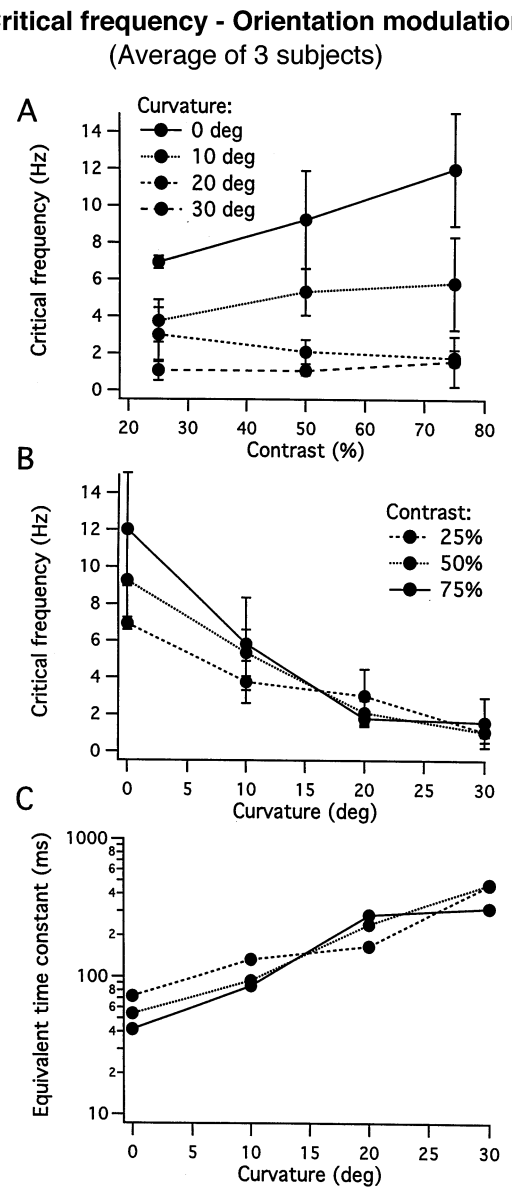

Fig. 6. Critical temporal frequency for orientation modulation derived from the fits shown in Fig. 5. Critical frequency: (A) as a function of contrast for each curvature; (B) as a function of curvature for each contrast; (C) critical duration for the test part of the stimuli. Each data point represents the mean for the three subjects. Error bars denote S.D.

$$PC(x) = pc_{\max} - (pc_{\max} - 50) \times e^{-(x/T)^{\beta}} \quad (2)$$

where PC is percent correct, $pc_{\max}$ is the asymptotic performance level, T is the critical duration (corresponding to a relative increase of $(1 - 1/e)\%$), β is the slope, and x is duration. Thus,

$$PC(T) = (pc_{\max} - 50)*0.63 + 50$$

Fig. 4 shows critical durations derived from averaging the fits across the three subjects as a function of contrast (Fig. 4A) and curvature (Fig. 4B), respectively. In Fig. 4A critical duration as a function of contrast is approximately constant; there is no clear dependence on contrast. However, the critical duration increases with the curvature of the contour (Fig. 4B). A Friedman's two-way ANOVA for each curvature condition confirms that there is no significant main effect of contrast on critical duration for contour integration, and a Friedman's two-way ANOVA on the data pooled across contrast conditions shows that there is a significant main effect of curvature ($X^2_F = 27.109$, df = 3, $P < 0.0001$, $N = 12$). A Wilcoxon signed rank test (5% significance level) shows there are significant differences in critical duration between all curvature conditions, except for the higher curvatures (20 and 30°), the critical durations for lower curvatures being 150–200 ms shorter than those for higher curvatures.

The difference in the extent to which contour curvature affects the initial rise in performance at short durations between the non-masked and masked conditions (Figs. 2 and 3) demonstrates the adequacy of the mask for preventing the continued processing of path detection after the disappearance of a briefly presented test stimulus. The experiment in which a mask was used also demonstrates that curvature has a stronger effect on path detection than contrast. Path detection needs more processing time with the increase of curvature, suggesting that path detection is not performed through a set of static filters (i.e. without temporal dependence).

3.2. Effect of temporally modulating the orientation of the individual elements

In the second experiment, we tested the effect of temporally modulating the orientation of individual elements of the stimuli (path and background) in a temporal sequence to make and break contour linking while keeping all other factors constant. This is essentially a steady-state version of experiment 1 but it also allows an assessment of the importance of multi-cycle presentations. Detection was measured over a range of temporal frequencies (0.5–19 Hz), contrasts (25–75%), and path curvatures (0–30°). 19 Hz was the highest temporal frequency used, and 0.5 Hz the lowest. Note that at 0.5 Hz only the contour stimulus can be presented under the temporal Gaussian window of 1 s (i.e. no non-contour mask is presented). Typical data for one subject are shown in Fig. 5, solid curves denote fits as described below. Each curve represents performance on path detection as a function of the temporal frequency of element rotation for each contrast and each curvature.

Performance for path detection decreases smoothly with temporal frequency. Similar to the first experiment, contrast does not significantly affect this decrease while increase in curvature does significantly affects maximum performance (at 0.5 Hz). To quantify the temporal limits on performance we calculated critical

temporal frequencies for path detection by fitting the data of Fig. 5 (performance as a function of temporal frequency at each path curvature and each contrast) with a Weibull function corrected to take the differing asymptotic levels into account:

$$PC(x) = 50 + (pc_{\max} - 50) \times e^{-(x/F)^{\beta}} \quad (3)$$

where PC is percent correct, $pc_{\max}$ is the asymptotic performance level, F is the critical frequency, β is the slope, and x is temporal frequency. The critical frequency (F) of this function is 1/e% of the asymptotic level relative to guess level, and it was corrected back to $(1 - 1/e)$% for comparison with experiment 1 with the formula: $A = F.\ [-\ln(1 - e^{-1})]^{1/\beta}$.

Fig. 6A shows these critical frequencies derived from averaging the fits to the data of our three subjects as a function of contrast. Contrast has little effect on the critical frequency for orientation modulation in time. Fig. 6B shows critical frequencies as a function of curvature again averaged across the three subjects' data. The critical frequency for orientation modulation clearly declines with curvature. A Friedman's two-way ANOVA for each curvature condition confirms that there is no significant main effect of contrast on critical frequency of orientation modulation, and a Friedman's two-way ANOVA on the data pooled across contrast conditions confirms that there is a significant main effect of curvature ($X_F^2 = 23.8$, df = 3, $P < 0.0001$, $N = 9$). A Wilcoxon signed rank test (5% significance level) shows there are significant differences between all curvature conditions, except between the two highest (20 and 30°): critical frequency decreases steeply with curvature (from 9.5 ± 3.5 Hz for straight paths) to reach an asymptotic level (1.2 ± 0.9 Hz) around 30° of curvature. This result suggests that, similar to the critical duration found for the masked condition in experiment 1, critical temporal frequency for path detection is not fixed but depends on curvature. From these critical temporal frequencies one can also derive equivalent time constants for the contour stimulus using the relation:

$$T = 1/(2*F)$$

Fig. 6C shows the critical duration (derived from the critical frequency averaged across subjects) for the contour stimulus as a function of curvature and at different contrasts: test critical duration increases smoothly with curvature. Interestingly, the critical duration in the

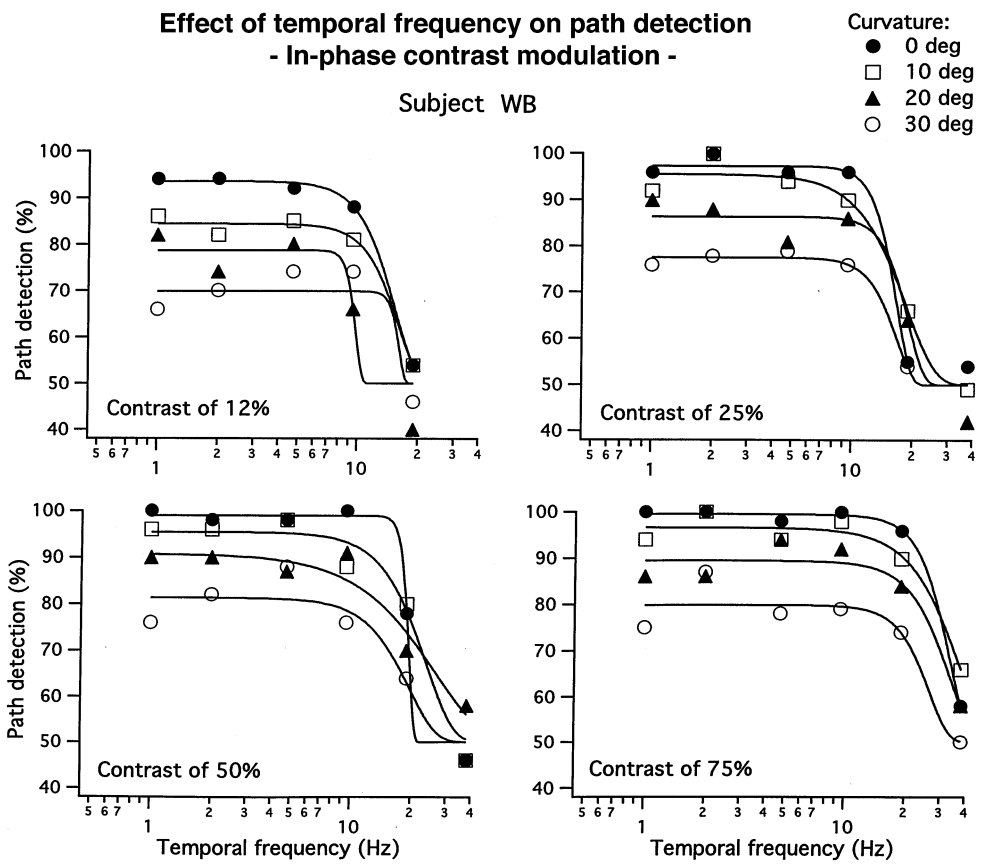

Fig. 7. Effect of curvature and contrast on path detection as a function of stimulus temporal frequency in the temporal contrast modulation experiment (in-phase condition). Data shown for one subject (WB), other subjects show similar results. Each subject performs one to three sessions of 50 trials per data point. Filled and open symbols represent performance measurement (% correct). Solid lines denote fits to Eq. (3) for each data set.

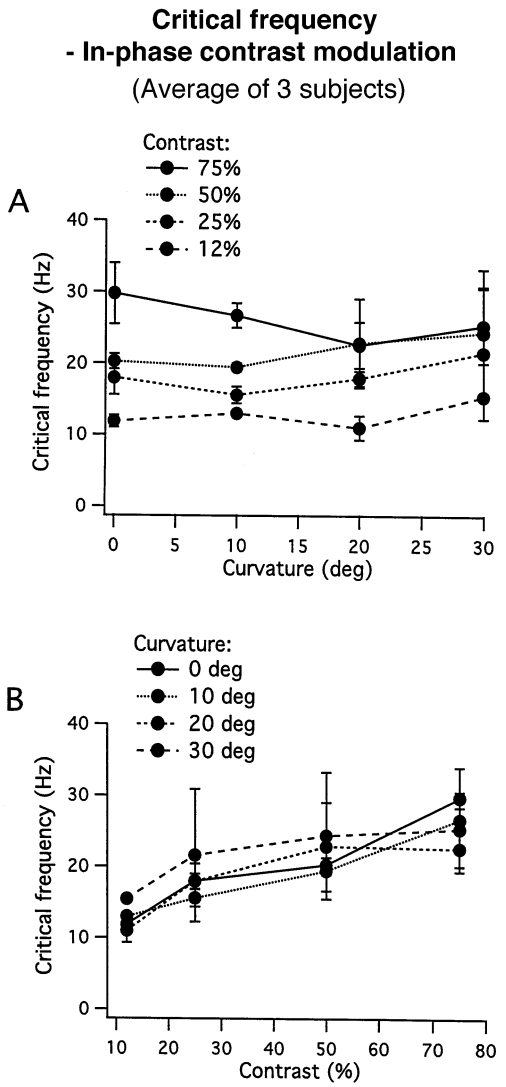

Fig. 8. Critical temporal frequencies for contrast modulation derived from the fits shown in Fig. 7. Critical frequencies: (A) as a function of curvature for each contrast; (B) as a function of contrast for each curvature. Each data point represents the mean for the three subjects. Error bars denote S.D.

steady-state, flickering condition are very similar to those measured in experiment 1 (Fig. 4B, masked condition) and shown in Fig. 4B (50–400 ms depending on curvature).

3.3. Effect of temporally modulating the contrast of the individual elements

To gauge the extent to which the visibility of individual Gabor elements limited performance in the preceding experiments, contour integration was measured for temporally modulated (same spatial phase) Gabor elements. In this experiment, we looked at the effect of temporally modulating the contrast of the individual elements of our stimulus (i.e. contrast-reversal of all the elements comprising the path and background). Contrast polarity alternated and the orientation of individual elements remained constant. In order to delineate how contrast is temporally and spatially integrated by the linking process, performance was tested under two different conditions: in one condition paths were composed of in-phase Gabor patches, and in another each alternate path element was 180° out of phase both spatially and temporally. In an identical manner to experiment 2, path detection was measured over a range of temporal frequency (0.5–38 Hz), achromatic cone contrasts (25–75%), and path curvatures (0–30°). At 0.5 Hz only one stimulus frame is presented under the temporal Gaussian window of 1 s (i.e. no contrast reversal). Representative results in the in-phase condition for one of the three subjects tested are shown in Fig. 7 by data points, solid curves denote fits as described below. Each curve represents performance of path detection as a function of temporal frequency for each contrast and each curvature.

Below 10 Hz, performance reaches an *asymptotic* level whose magnitude depends on curvature but is relatively independent of contrast. Regardless of either the contrast or curvature, psychometric performance decreases with temporal frequency above 10 Hz. This may be attributed either to the decrease of perceived contrast with the increase of temporal frequency or to the temporal limitation of the linking process itself, or to both. These effects were quantified by fitting the data of Fig. 7 with Eq. (3), previously used in experiment 2. Fig. 8A and B show critical frequencies (averaged fits for the three subjects) as a function of curvature and contrast, respectively. A Friedman's two-way ANOVA for each contrast condition shows that there is no significant main effect of curvature on critical frequency for contrast modulation, and a Friedman's two-way ANOVA on the data pooled across curvature conditions shows that there is a clear main effect of contrast ($X^2_F = 18.943$, df = 3, $P = 0.0003$, $N = 12$). A Wilcoxon signed rank test (5% significance level) shows there are significant differences between all contrast conditions, except for the higher contrasts (50 and 75%): critical frequency increases significantly with contrast from 12.4 ± 1.9 Hz at 12% to 25.5 ± 2.5 Hz at 75%.

Contrary to experiment 2 in which critical frequencies for orientation modulation strongly depend on curvature not contrast, here the critical frequencies are contrast not curvature-dependent when contrast-reversal of individual elements is used. Critical frequency is noticeably better (i.e. has a better time resolution) when the contrast rather than the orientation of individual elements is modulated.

Figs. 9 and 10 show the result in the anti-phase condition for one subject WB and for two contrasts (50–75%). Critical frequency is relatively invariant with curvature for both 75% and 50%, similar to the in-

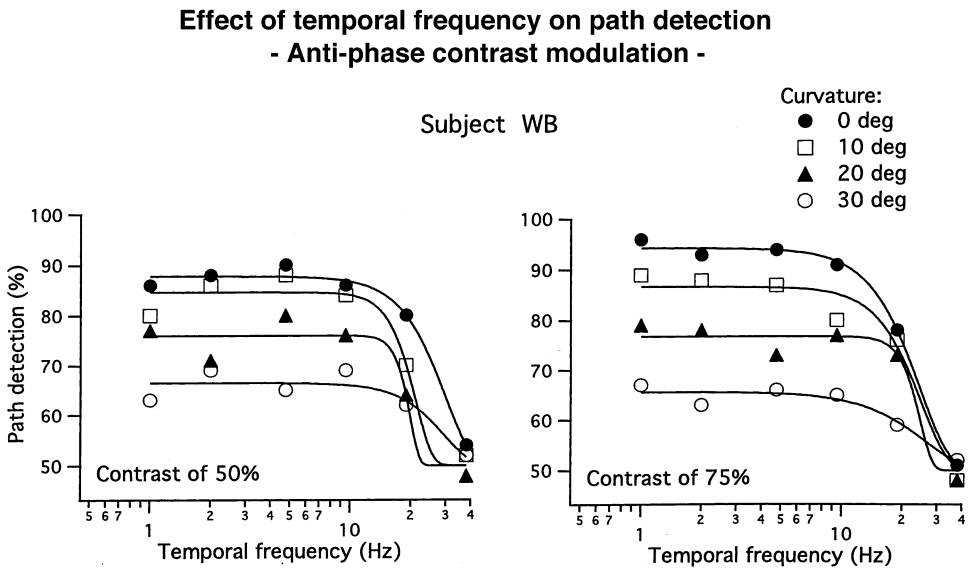

Fig. 9. Effect of curvature and contrast on path detection as a function of stimulus temporal frequency in the temporal contrast modulation experiment (anti-phase condition). The number of trials was 50–150 per data point (subject WB only). Filled and open symbols represent performance measurement (% correct). Solid lines denote fits to Eq. (3) for each data set.

phase condition (Fig. 8A). Change in contrast polarity along the contour decreases asymptotic performance (compare Figs. 7 and 9), but does not affect significantly the critical frequency for contrast modulation (20–25 Hz). The effect of the change in contrast polarity along the path is consistent with that of previous studies (McIlhagga & Mullen, 1996; Mullen et al., 2000; Field, Hayes, & Hess, 2000). Thus, change in contrast polarity disrupts contour extraction but not its contrast-dependent dynamics. This implies that the association field is more sensitive to the spatial phase than to the temporal phase of contrast since spatial phase alternation disrupts the orientation linking more than does temporal phase alternation. Consequently, the contrast-dependent dynamics reported in these experiments do not reflect the dynamics of contour integration as a whole but rather the dynamics associated with the processing of the individual elements comprising the contour.

4. Discussion

The main finding is that there are dynamics to contour integration: contour integration is slower for more curved contours (Exps 1 & 2). This is consistent with a current study showing a dependence of reaction times for contour processing on curvature (Beaudot & Mullen, forthcoming & personal communication). The critical frequency which is a measure of temporal acuity was around 10 Hz for straight contours but only around 1–2 Hz for curved contours (30° path angle), with a continuous change between these two extremes (Exp 2). The contours that were used in the main study were jagged ones but it has also been verified that smooth contours exhibited similar temporal dependencies (see Table 1). In agreement with Elder and Zucker (1993), who measured reaction times for detection of localized elements in a visual search paradigm, it was found that closed contours (smooth curvature of 36° for ten elements) are detected faster than open contours with the same curvature by about a factor of 2 (Table 1). It is interesting that this speed advantage for closed contours was not reflected in a higher asymptotic performance (see Table 1) despite the fact that closed

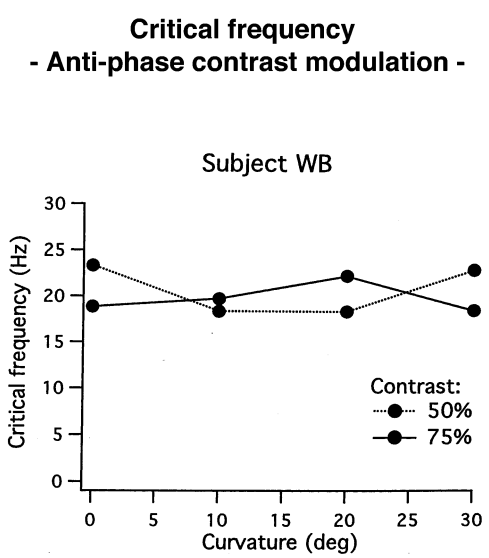

Fig. 10. Critical temporal frequencies derived from the fits shown in Fig. 9 as a function of curvature for each contrast (subject WB only).

Table 1
Summary measures from three subjects for jagged, smooth and closed contours[a]

Path	Subjects	Critical frequency	Asymptotic level
Jagged (30°)	RFH	0.720703	69.848
	WB	0.966041	81.839
	KTM	3.50782	83.805
	Mean ± S.D.	1.732 ± 1.261	78.497 ± 6.168
Smooth (30°)	RFH	1.16089	74
	WB	3.19773	76.055
	KTM	0.890552	84
	Mean ± S.D.	1.75 ± 1.03	78.018 ± 4.312
Closed (36°)	RFH	1.32289	81
	WB	5.93353	82.449
	KTM	4.73703	79
	Mean ± S.D.	3.998 ± 1.953	80.816 ± 1.414

[a] The dynamics for closed contours is a factor of two better than for open ones, though their asymptotic levels are similar.

contours are generally more detectable than open ones (Kovacs & Julesz, 1993; Pettet, McKee, & Grzywacz, 1998; Braun, 1999).

The finding that curved contours take longer to detect than straight ones suggests two things. First, it is unlikely that contours of different curvature are each detected by dedicated detectors but rather in a flexible and distributed population code. Second, the finding suggests that path detection could result from a dynamic process, intrinsically tuned to straight paths (curvature of 0°) and evolving temporally to a curvature tuning matching the spatial properties of the path. Such a process may depend on intra- and extra-cortical feedback known to be important in contextual modulation and figure-ground segregation (Gilbert & Wiesel, 1990; Burkhalter, 1993; Kapadia, Ito, Gilbert, & Westheimer, 1995; Sillito, Grieve, Jones, Cudeiro, & Davis, 1995; Fregnac, Bringuier, & Chavane, 1996; Fregnac et al., 1996; Gilbert, 1996; Gilbert et al., 1996; Sillito & Jones, 1996; Toth et al., 1996; Adini, Sagi, & Tsodyks, 1997; Levitt & Lund, 1997; Gilbert, 1998; Hupé et al., 1998; Lamme, Zipser & Spekreijse, 1998; Lamme et al., 1998; Das & Gilbert, 1999; Hess & Field, 1999; Kapadia et al., 1999; Polat, 1999).

The similarity in time constants between one-shot and multi-shot presentations (comparison of results for Exps 1 & 2) of the same stimulus in which the orientation of individual elements is cyclically varied suggests that repeated presentations (with a 500 ms Gaussian modulation in a 1 s window) bring no improvement over a simple one-shot presentation. The mechanism involved in linking orientations across space must not benefit from a repeated presentation of the same stimulus. Therefore, linking has to be a short-term process, with an integration time dependent on curvature, triggered by the stimulus presentation, and efficiently broken down by a mask disrupting the visual linking (orientation continuity). This suggests a mechanism that is not highly reliant on iterative processing to achieve optimum performance. For example, this finding rules out the possibility that orientation linking is followed by a slow integration stage through which an iterative process could enhance performance when multiple stimulus cycles are presented.

Two lines of evidence suggest there are two different underlying processes limiting performance on this contour detection paradigm, one involving the dynamics associated with the processing of the array elements per se, as assessed by modulating their contrast and another involving the dynamics associated with the detection of the contour that they comprise, as assessed by modulating element orientation. Firstly, the temporal resolution of element processing is high (20–30 Hz at high contrasts) and does not depend on contour curvature (Exp 3), whereas the temporal resolution of contour processing is very low (2–12 Hz) and is strongly curvature dependent (Exps 1 & 2). Secondly, the finding that the critical frequency for detecting individual elements is contrast dependent while the critical frequency for detecting the contour is not, suggests separate processes. The superior temporal resolution of element detection may represent the initial feedforward input to the network that carries the code for contrast (Gawne, Kjaer, & Richmond, 1996; Richmond et al., 1997; Lamme et al., 1998; Hess et al., 1998), the slower temporal resolution of contour detection, the outcome of intra- and extra-cortical feedback processes which carry the code for contour detection independent of the absolute level or relative polarity of the contrast of its constituents (Lamme, 1995; Zipser et al., 1996; Richmond et al., 1997; Hess et al., 1998; Lamme et al., 1998).

The results do not rule out the possibility that feature binding is accomplished by synchronous oscillations (i.e. the hypothesis of Singer and colleagues). Investigation of the temporal properties of neural oscillatory synchronization in cat striate cortex (Gray, Engel, Konig, & Singer, 1992) showed that duration of synchrony is variable (100–900 ms) and that phase differences and frequencies of synchronized events are also variable (± 3 ms, 40–60 Hz), suggesting a high degree of dynamic variability and a rapid onset and offset of synchrony among interacting populations of neurons. However, if the synchronicity of cortical oscillations determines feature binding in contour integration, this process must require many temporal cycles to work (i.e. relatively slow dynamics) and for reasons yet unknown this requirement must increase for more curved contours.

Current models of contour integration (Heitger, Rosenthaler, von der Heydt, Peterhans, & Kubler, 1992; Williams & Jacobs, 1997; Li, 1998; Yen & Finkel,

1998; Grossberg, 1999; Li, 1999) have yet to incorporate explicitly any dynamics.

Acknowledgements

This study was funded by grants from the Medical Research Council of Canada to K.T. Mullen (MT-10819) and R.F. Hess (MT-10818), and partially supported by a fellowship from the Fyssen Foundation to W.H.A. Beaudot. We also acknowledge partial support from the 'Réseau FRSQ de Recherche en Santé de la Vision'.

References

Adini, Y., Sagi, D., & Tsodyks, M. (1997). Excitatory-inhibitory network in the visual cortex: psychophysical evidence. *Proceedings of the National Academy of Sciences of the United States of America*, *94*, 10426–10431.

Alais, D., Blake, R., & Lee, S. H. (1998). Visual features that vary together over time group together over space. *Natural Neuroscience*, *1*, 160–164.

Atkinson, J., & Braddick, O. (1992). Visual segmentation of oriented textures by infants. *Behavioural Brain Research*, *49*, 123–131.

Beaudot, W. H. A. (forthcoming). Role of onset asynchrony in contour integration.

Beaudot, W. H. A., & Mullen, K. T. M. (forthcoming). Processing time of contour integration: The role of color, contrast and curvature.

Blake, R., & Yang, Y. (1997). Spatial and temporal coherence in perceptual binding. *Proceedings of the National Academy of Sciences of the United States of America*, *94*, 7115–7119.

Bosking, W. H., Zhang, Y., Schofield, B., & Fitzpatrick, D. (1997). Orientation selectivity and the arrangement of horizontal connections in tree shrew striate cortex. *Journal of Neuroscience*, *17*, 2112–2127.

Braun, J. (1999). On the detection of salient contours. *Spatial Vision*, *12*, 211–225.

Burkhalter, A. (1993). Development of forward and feedback connections between areas V1 and V2 of human visual cortex. *Cerebral Cortex*, *3*, 476–487.

Das, A., & Gilbert, C. D. (1999). Topography of contextual modulations mediated by short-range interactions in primary visual cortex. *Nature*, *399*, 655–661.

Elder, J., & Zucker, S. (1993). The effect of contour closure on the rapid discrimination of two-dimensional shapes. *Vision Research*, *33*, 981–991.

Fahle, M. (1993). Figure-ground discrimination from temporal information. *Proceedings of the Royal Society of London. Series B: Biological Sciences*, *254*, 199–203.

Field, D. J., Hayes, A., & Hess, R. F. (1993). Contour integration by the human visual system: evidence for a local 'association field'. *Vision Research*, *33*, 173–193.

Field, D. J., Hayes, A., & Hess, R. F. (2000). The roles of polarity and symmetry in the perceptual grouping of contour fragments. *Spatial Vision*, *13*, 51–66.

Fregnac, Y., Bringuier, V., & Chavane, F. (1996). Synaptic integration fields and associative plasticity of visual cortical cells in vivo. *Journal of Physiology Paris*, *90*, 367–372.

Fregnac, Y., Bringuier, V., Chavane, F., Glaeser, L., & Lorenceau, J. (1996). An intracellular study of space and time representation in primary visual cortical receptive fields. *Journal of Physiology Paris*, *90*, 189–197.

Gawne, T. J., Kjaer, T. W., & Richmond, B. J. (1996). Latency: another potential code for feature binding in striate cortex. *Journal of Neurophysiology*, *76*, 1356–1360.

Gilbert, C. D. (1996). Plasticity in visual perception and physiology. *Current Opinion in Neurobiology*, *6*, 269–274.

Gilbert, C. D. (1997). Cortical dynamics. *Acta Paediatrica. Supplement*, *422*, 34–37.

Gilbert, C. D. (1998). Adult cortical dynamics. *Physiological Reviews*, *78*, 467–485.

Gilbert, C. D., Das, A., Ito, M., Kapadia, M., & Westheimer, G. (1996). Spatial integration and cortical dynamics. *Proceedings of the National Academy of Sciences of the United States of America*, *93*, 615–622.

Gilbert, C. D., & Wiesel, T. N. (1983). Clustered intrinsic connections in cat visual cortex. *Journal of Neuroscience*, *3*, 1116–1133.

Gilbert, C. D., & Wiesel, T. N. (1989). Columnar specificity of intrinsic horizontal and corticocortical connections in cat visual cortex. *Journal of Neuroscience*, *9*, 2432–2442.

Gilbert, C. D., & Wiesel, T. N. (1990). The influence of contextual stimuli on the orientation selectivity of cells in primary visual cortex of the cat. *Vision Research*, *30*, 1689–1701.

Golledge, H. D. R., Hilgetag, C. C., & Tovee, M. J. (1996). A solution to the binding problem? Information processing. *Current Biology*, *6*, 1092–1095.

Gray, C. M., Engel, A. K., Konig, P., & Singer, W. (1992). Synchronization of oscillatory neuronal responses in cat striate cortex: temporal properties. *Visual Neuroscience*, *8*, 337–347.

Grossberg, S. (1999). How does the cerebral cortex work? Learning, attention, and grouping by the laminar circuits of visual cortex. *Spatial Vision*, *12*, 163–185.

Hardcastle, V. G. (1997). Consciousness and the neurobiology of perceptual binding. *Seminars in Neurology*, *17*, 163–170.

Heitger, F., Rosenthaler, L., von der Heydt, R., Peterhans, E., & Kubler, O. (1992). Simulation of neural contour mechanisms: from simple to end-stopped cells. *Vision Research*, *32*, 963–981.

Hess, R., & Field, D. (1999). Integration of contours: new insights. *Trends in Cognitive Science*, *3*, 480–486.

Hess, R. F., Dakin, S. C., & Field, D. J. (1998). The role of 'contrast enhancement' in the detection and appearance of visual contours. *Vision Research*, *38*, 783–787.

Hupé, J. M., James, A. C., Payne, B. R., Lomber, S. G., Girard, P., & Bullier, J. (1998). Cortical feedback improves discrimination between figure and background by V1, V2 and V3 neurons. *Nature*, *394*, 784–787.

Kapadia, M. K., Ito, M., Gilbert, C. D., & Westheimer, G. (1995). Improvement in visual sensitivity by changes in local context: parallel studies in human observers and in V1 of alert monkeys. *Neuron*, *15*, 843–856.

Kapadia, M. K., Westheimer, G., & Gilbert, C. D. (1999). Dynamics of spatial summation in primary visual cortex of alert monkeys. *Proceedings of the National Academy of Sciences of the United States of America*, *96*, 12073–12078.

Kiper, D. C., Gegenfurtner, K. R., & Movshon, J. A. (1996). Cortical oscillatory responses do not affect visual segmentation. *Vision Research*, *36*, 539–544.

Kovacs, I. (1996). Gestalten of today: early processing of visual contours and surfaces. *Behavioural Brain Research*, *82*, 1–11.

Kovacs, I., & Julesz, B. (1993). A closed curve is much more than an incomplete one: effect of closure in figure-ground segmentation. *Proceedings of the National Academy of Sciences of the United States of America*, *90*, 7495–7497.

Lamme, V. A. (1995). The neurophysiology of figure-ground segregation in primary visual cortex. *Journal of Neuroscience*, *15*, 1605–1615.

Lamme, V. A., & Spekreijse, H. (1998). Neuronal synchrony does not represent texture segregation. *Nature*, *396*, 362–366.

Lamme, V. A., Super, H., & Spekreijse, H. (1998). Feedforward, horizontal, and feedback processing in the visual cortex. *Current Opinion in Neurobiology*, *8*, 529–535.

Lamme, V. A., Zipser, K., & Spekreijse, H. (1998). Figure-ground activity in primary visual cortex is suppressed by anesthesia. *Proceedings of the National Academy of Sciences of the United States of America*, *95*, 3263–3268.

Lee, S. H., & Blake, R. (1999). Visual form created solely from temporal structure [see comments]. *Science*, *284*, 1165–1168.

Levitt, J. B., & Lund, J. S. (1997). Contrast dependence of contextual effects in primate visual cortex. *Nature*, *387*, 73–76.

Li, Z. (1998). A neural model of contour integration in the primary visual cortex. *Neural Computation*, *10*, 903–940.

Li, Z. (1999). Visual segmentation by contextual influences via intracortical interactions in the primary visual cortex. *Network-Computation in Neural Systems*, *10*, 187–212.

Lorenceau, J., & Zago, L. (1999). Cooperative and competitive spatial interactions in motion integration. *Visual Neuroscience*, *16*, 755–770.

Malach, R., Amir, Y., Harel, M., & Grinvald, A. (1993). Relationship between intrinsic connections and functional architecture revealed by optical imaging and in vivo targeted biocytin injections in primate striate cortex. *Proceedings of the National Academy of Sciences of the United States of America*, *90*, 10469–10473.

McIlhagga, W. H., & Mullen, K. T. (1996). Contour integration with colour and luminance contrast. *Vision Research*, *36*, 1265–1279.

Mullen, K. T. M., Beaudot, W. H. A., & McIlhagga, W. H. (2000). Contour integration in color vision: a common process for the blue-yellow, red-green and luminance mechanisms? *Vision Research*, *40*, 639–655.

Pettet, M. W. (1999). Shape and contour detection. *Vision Research*, *39*, 551–557.

Pettet, M. W., McKee, S. P., & Grzywacz, N. M. (1998). Constraints on long range interactions mediating contour detection. *Vision Research*, *38*, 865–879.

Polat, U. (1999). Functional architecture of long-range perceptual interactions. *Spatial Vision*, *12*, 143–162.

Richmond, B. J., Gawne, T. J., & Jin, G. X. (1997). Neuronal codes: reading them and learning how their structure influences network organization. *Biosystems*, *40*, 149–157.

Rockland, K. S., & Lund, J. S. (1982). Widespread periodic intrinsic connections in the tree shrew visual cortex. *Science*, *215*, 1532–1534.

Roelfsema, P. R., & Singer, W. (1998). Detecting connectedness. *Cerebral Cortex*, *8*, 385–396.

Sillito, A. M., Grieve, K. L., Jones, H. E., Cudeiro, J., & Davis, J. (1995). Visual cortical mechanisms detecting focal orientation discontinuities. *Nature*, *378*, 492–496.

Sillito, A. M., & Jones, H. E. (1996). Context-dependent interactions and visual processing in V1. *Journal of Physiology Paris*, *90*, 205–209.

Singer, W., & Gray, C. M. (1995). Visual feature integration and the temporal correlation hypothesis. *Annual Review of Neuroscience*, *18*, 555–586.

Toth, L. J., Rao, S. C., Kim, D. S., Somers, D., & Sur, M. (1996). Subthreshold facilitation and suppression in primary visual cortex revealed by intrinsic signal imaging. *Proceedings of the National Academy of Sciences of the United States of America*, *93*, 9869–9874.

Usher, M., & Donnelly, N. (1998). Visual synchrony affects binding and segmentation in perception. *Nature*, *394*, 179–182.

Williams, L. R., & Jacobs, D. W. (1997). Stochastic completion fields; a neural model of illusory contour shape and salience. *Neural Computation*, *9*, 837–858.

Yen, S. C., & Finkel, L. H. (1998). Extraction of perceptually salient contours by striate cortical networks. *Vision Research*, *38*, 719–741.

Ziebell, O., & Nothdurft, H. C. (1999). Cueing and pop-out. *Vision Research*, *39*, 2113–2125.

Zipser, K., Lamme, V. A., & Schiller, P. H. (1996). Contextual modulation in primary visual cortex. *Journal of Neuroscience*, *16*, 7376–7389.